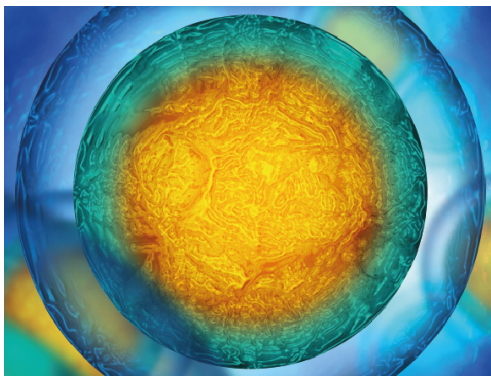


PAPER

Protrusion mechanism study in sipunculid worms as model for developing bio-inspired linear actuators

To cite this article: Silvia Filogna *et al* 2021 *Bioinspir. Biomim.* **16** 026008

View the [article online](#) for updates and enhancements.



Biophysical Society

IOP | ebooks™

Your publishing choice in all areas of biophysics research.

Start exploring the collection—download the first chapter of every title for free.

Bioinspiration & Biomimetics



PAPER

Protrusion mechanism study in sipunculid worms as model for developing bio-inspired linear actuators

RECEIVED
31 July 2020

REVISED
21 October 2020

ACCEPTED FOR PUBLICATION
30 October 2020

PUBLISHED
18 December 2020

Silvia Filogna^{1,2,*} , Veronica Iacovacci^{1,2} , Fabrizio Vecchi³ , Luigi Musco³  and Arianna Menciassi^{1,2} 

¹ The BioRobotics Institute, Scuola Superiore Sant'Anna, Pisa, Italy

² Department of Excellence in Robotics & AI, Scuola Superiore Sant'Anna, Pisa, Italy

³ Stazione Zoologica Anton Dohrn, Napoli, Italy

* Address for correspondence: The BioRobotics Institute, viale Rinaldo Piaggio 34, 56025 Pontedera, Pisa, Italy

E-mail: silvia.filogna@santannapisa.it, veronica.iacovacci@santannapisa.it, fabrizio.vecchi@szn.it, luigi.musco@szn.it and arianna.menciassi@santannapisa.it

Keywords: worm biomechanics, bio-inspired robotics, protrusion force

Abstract

The invertebrates ability to adapt to the environment during motion represents an intriguing feature to inspire robotic systems. We analysed the sipunculid species *Phascolosoma stephensoni* (Sipunculidae, Annelida), and quantitatively studied the motion behaviour of this unsegmented worm. The hydrostatic skeleton and the muscle activity make the infaunal *P. stephensoni* able to extrude part of its body (the introvert) from its burrow to explore the environment by remaining hidden within the rocky substrate where it settled. The introvert protrusion is associated with changes in the body shape while keeping the overall volume constant. In this study, we employed a marker-less optical tracking strategy to quantitatively study introvert protrusion (i.e. kinematics, elongation percentage and forces exerted) in different navigation media. When *P. stephensoni* specimens were free in sea water (outside from the burrow), the worms reached lengths up to three times their initial ones after protrusion. Moreover, they were able to elongate their introvert inside a viscous medium such as agar-based hydrogel. In this case, the organisms were able to break the hydrogel material, exerting forces up to 3 N and then to navigate easily inside it, producing stresses of some tens of kPa. Our measurements can be used as guidelines and specifications to design and develop novel smart robotic systems.

1. Introduction

Biological diversity captures researchers' attention as a great source of inspiration for finding new solutions to engineering and technological problems. This applies also to robotics that constantly struggles to develop smart machines able to navigate and adapt in unstructured environment [1]. Different application scenarios, ranging from exploration and rescue tasks to surgery, call for robots able to move efficiently in the surroundings, avoiding obstacles and reaching targets in a safe way. Despite the design of artifacts featured by these abilities is not straightforward, some continuum robots have been developed for industrial and space applications [2] as well as for medical ones, as in the case of concentric tubes and steerable needles [3]. Depending on the employed actuation principles, these tools present some drawbacks such as difficulties in miniaturization, in performing complex tasks and

in force sensing. Moreover, small-scales devices witness particular limitations in deployment and target reaching [4].

Over the past years, the phylum Annelida has represented an intriguing source of inspiration for the development of novel machines, due to the capability of these organisms to adapt to different habitats and to their simplified—yet effective—motor abilities [5]. Several research groups have focused on the analysis of the earthworm crawling kinematics [6–12], providing quantitative data useful to realize bioinspired artifacts. Indeed, in the last two decades, a large number of worm-like prototypes have been implemented for real-world applications, wherever adaptability to complex environment was required, e.g. for minimally invasive medical procedures. Many attempts have been made to design, fabricate and model the peristaltic locomotion of different annelid species [13–18] and various actuation approaches

have been proposed. In the literature, at least four actuation strategies have been identified, spanning from electromagnetic actuators [19, 20], smart materials (i.e. shape memory alloys and dielectric actuators) [21–25], fluidic [26] and piezoelectric actuators [27]. Each of the proposed solutions presents disadvantages, such as the slow response of shape memory alloys, the piping problem in fluidic systems and the micrometer-order displacement of piezoelectric actuators [15]. The development of peristaltic robotic analogues has been prevented by the lack of suitable linear actuators with muscle-like properties [28] and modular control [29]. To date, soft actuators offer solutions for narrow space applications, taking advantages of the flexibility of soft materials [30–33].

In order to overcome some of these limitations, especially those affecting systems downscaling, and to implement novel deployment mechanisms, we can take inspiration from sipunculid worms, a more simplified Annelida taxon. Although annelids are segmented worms, the evolution led to the loss of the body segmentation in sipunculids. This Annelida taxon presents a continuum body and the ability to carry out an interesting and unique movement strategy based on a fluid-filled body (trunk) and a retractable proboscis (introvert) [34] (figure 1(a)). Sipunculids explore the surroundings by protruding and elongating the introvert (protrusion configuration), whereas they retract their body to escape predators or as a reaction to external stimuli (defence configuration) [35] (figure 1(b)). However, Murina described four different ecological groups of sipunculans based on their feeding modes and mobility. Among these groups, the sipunculid species living in holes or crevices of rocks or other hard materials, such as *Phascolosoma stephensoni* (Stephen, 1942), are able to explore the surrounding surface from a fixed position by protruding the introvert and scrape-off/collect the deposited organic material, being these species surface deposit feeders [36]. Another ecological group of sipunculans is represented by species living in soft sediments (e.g. sand, silt/clay), such as *Sipunculus nudus* (Linnaeus, 1766). In these species the introvert protrusion is also used to burrow inside sediments where they search for buried organic material, causing sediment bioturbation, being these species, instead, subsurface deposit feeders [36–38]. This motor abilities are enabled by the synergistic action of circular/longitudinal muscles and of the hydrostatic skeleton without volume changes. This implies that every modification in length is reflected in a diameter variation [39–41] (figure 1(c)).

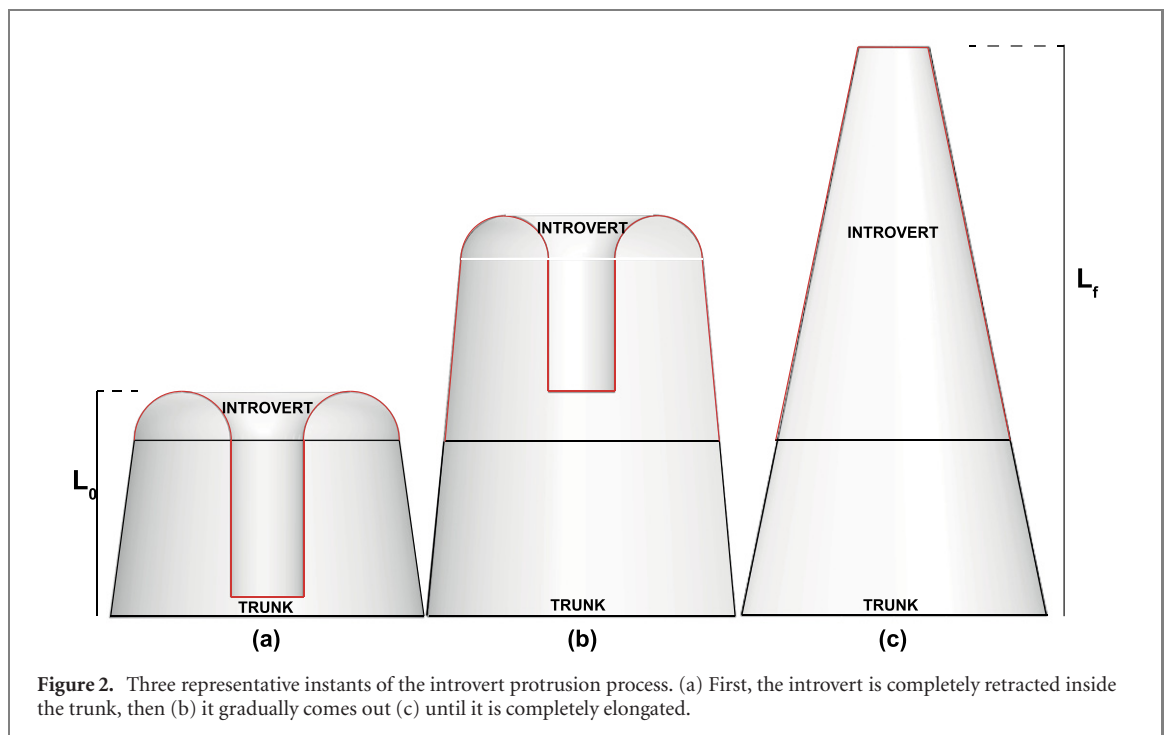
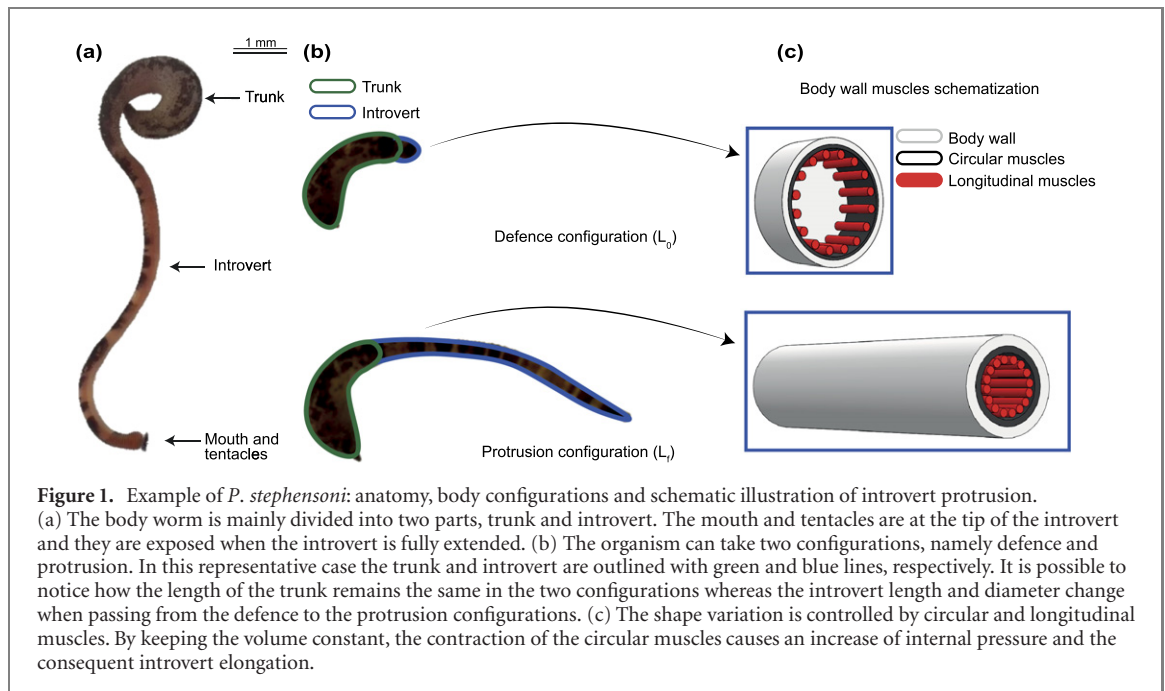
In particular, the protrusion mechanism consists in a gradual lengthening of the introvert from the trunk in which it is folded in. Figure 2 shows three-time instants during which the introvert is coming out. At the beginning, it is completely contained within the trunk (figure 2(a)), but the increase of

the internal pressure (due to the contraction of the circular muscles) enables the introvert elongation (figures 2(b) and (c)).

A protrusion mechanism like this could provide new hints to develop innovative bio-inspired machines. In general, to develop bio-inspired robotic artifacts, a quantitative characterization of the inspiring biological organisms is required, both in terms of displacements and forces. Optical methods are the most straightforward to analyse the organisms movements: both marker-based and marker-less tracking systems have been proposed in the state of the art [42]. In these works, the organisms locomotion has been video recorded and some markers have been applied on specific locations to enhance the visibility or highlight specific body parts [43–45]. Despite a marker-based approach facilitates the video analysis and allows for a better investigation of the locomotion, it creates artifacts or inhibits natural movement in small species. For this reason, dedicated marker-less optical tracking systems have been proposed. In particular, a 3D worm tracker and an image-processing algorithm have been developed to determine the trajectory and the kinematics of a terrestrial nematode (*Caenorhabditis elegans*) [46]. As mentioned, for a full characterization, the evaluation of the forces exerted is also necessary. Several studies have measured forces in various ways, including their estimation when burrowing in a gelatin medium [47–50]. Furthermore, burrowing forces were also measured in sipunculids, particularly in *S. nudus*. Forces were determined invasively through the insertion of a needle connected to a pressure transducer. From pressure and body cross-sectional area it has been possible to derive the force values produced by the animal during burrowing [37].

To the best of authors knowledge, in the literature there are no studies characterizing the protrusion mechanism and force in non-burrowing sipunculid species living inside rocks, such as *P. stephensoni*. The aim of our study is to shed light on this interesting biological mechanism in order to derive numerical parameters to design a new generation of small-scale continuum robots able to adopt deployment strategies.

In this paper, we focus on the sipunculid species *P. stephensoni* to quantify the introvert elongation percentage, the kinematics and the forces generated during eversion, by exploiting marker-less based tracking methods both in sea water and in viscous medium. This paper is organized as follows. Section 2 describes the proposed methods for characterization. Section 3 presents the results of the work, which are successively discussed in section 4.



2. Materials and methods

2.1. The model organism

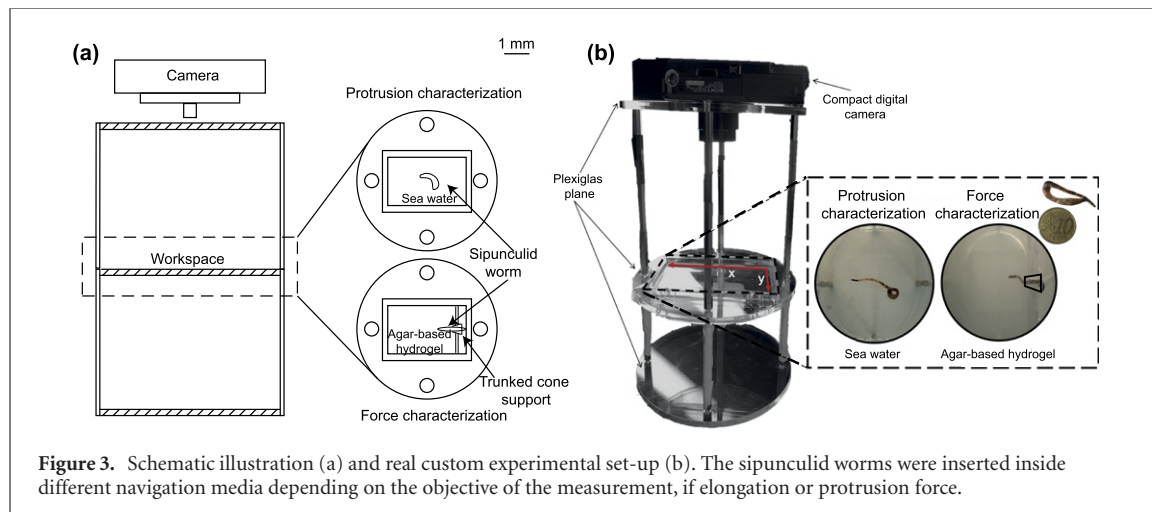
P. stephensoni is a widespread sipunculan species inhabiting hard substrata being usually found among crevices of rocks, seagrass meadows rhizomes, mussel beds and algae, including coralline algae. This species has a worldwide distribution and it is also commonly found in shallow waters in the Mediterranean area [51].

P. stephensoni specimens were collected from shallow rocks (30–50 cm deep) covered by coralline

algae (namely *Ellisolandia elongata*) in the Gulf of Naples (western Mediterranean Sea, Italy) from artificial boulders along the Chiaia shoreline (Naples), using hammer and chisel to scrape off the substrate. Upon collection, the material was transported to the facilities of the Stazione Zoologica Anton Dohrn (Naples, Italy) within sea water, where the worms were rapidly and gently sorted from rocks. After the sampling, worms were kept alive in sea water tanks containing stones, allowing the worms to shelter as in their native environment.

Table 1. Overview of organisms' features. Three samples are averaged for each group.

Group	L_0 (mm)	Diameter (mm)	Mass (mg)	Volume (mm ³)
1. Large	12.3 ± 2.3	4.0 ± 1.3	185.3 ± 0.6	130.3 ± 16.8
2. Medium	10.3 ± 1.5	2.5 ± 0.3	99.0 ± 2.6	49.4 ± 6.2
3. Small	8.3 ± 1.5	2.2 ± 0.65	26.3 ± 2.5	32.9 ± 4.81

**Figure 3.** Schematic illustration (a) and real custom experimental set-up (b). The sipunculid worms were inserted inside different navigation media depending on the objective of the measurement, if elongation or protrusion force.

Nine specimens were considered in this study and clustered in three groups based on their body dimensions that appeared naturally variable (table 1). In order to determine the morphometric parameters of the organisms and to divide them into groups, the initial length (L_0), trunk diameter, mass and volume of each worm were measured. Body length and diameter were evaluated through measuring tool (i.e. caliper) and confirmed by video recording data analysis. Worms wet weight was assessed through a digital precision scale. Volume measurements were performed through video recording data analysis and reported in table 1.

2.2. Experimental characterization set-up

Worms kinematics, elongation and penetration force were experimentally quantified thanks to a dedicated custom set-up. In order to enable proper optical tracking of the sipunculids in different media, the set-up was provided with a stable camera support and with a slot for the navigation arena (to be changed according to the medium). The set-up consisted of three stacked Plexiglas[®] layers (diameter 125 mm, thickness 3 mm) for the camera (top), the navigation arena (central) and for the structural base (bottom), respectively. They were properly shaped through laser cutting (Versalaser ILS series, Universal laser systems, East Paradise Lane, Scottsdale, USA) and connected through metallic spacers. The top plane was ring-shaped (central hole 44 mm diameter) to allow camera lodging. The central plane included a rectangular slot (length 90 mm and width 70 mm) housing the organisms during the tasks in different media

(figure 3). In particular, the worms were free to move in sea water during elongation characterization tests, whereas they protruded within agar hydrogels (featured by different concentrations) while quantifying eversion forces. In these tests, sipunculids were let anchoring their body in a dedicated support (trunked cone shaped) connected to the navigation arena, and then an additional Plexiglas[®] layer (thickness 1 mm) was placed on the top of the gel surface in order to avoid organisms to escape.

P. stephensoni specimens were filmed during tests via a compact digital camera (Cyber-shot DSC-W300 series, Sony, Minato-ku, Tokyo, Japan) with 13.6 megapixels lens (Carl Zeiss, Oberkochen, Germany) and 1/1.7" ($\sim 7.53 \times 5.64$ mm) CCD sensor. Videos were recorded digitally and stored on a microSD. A computer assisted analysis was performed through an open source software for tracking (Tracker video analysis and modelling tool, version 5.1.0, Open Source Physics in Java framework, Oracle Corporation, Redwood Shores, California, USA) which enabled to dynamically follow the coordinates of virtual markers placed by the operator on the body of the organism. The software automatically and continuously tracked the outermost frontal point of the introvert. Since the outermost point changes over time due to the gradual protrusion of the proboscis from the body, it was necessary to manually increase the number of virtual markers to determine the elongation trajectory. On the other hand, during the retraction, the tip was always represented by the outermost introvert point, thus enabling an easier tracking and trajectory reconstruction. With this method, we analysed the trajectories defined by the introvert on the plane, by

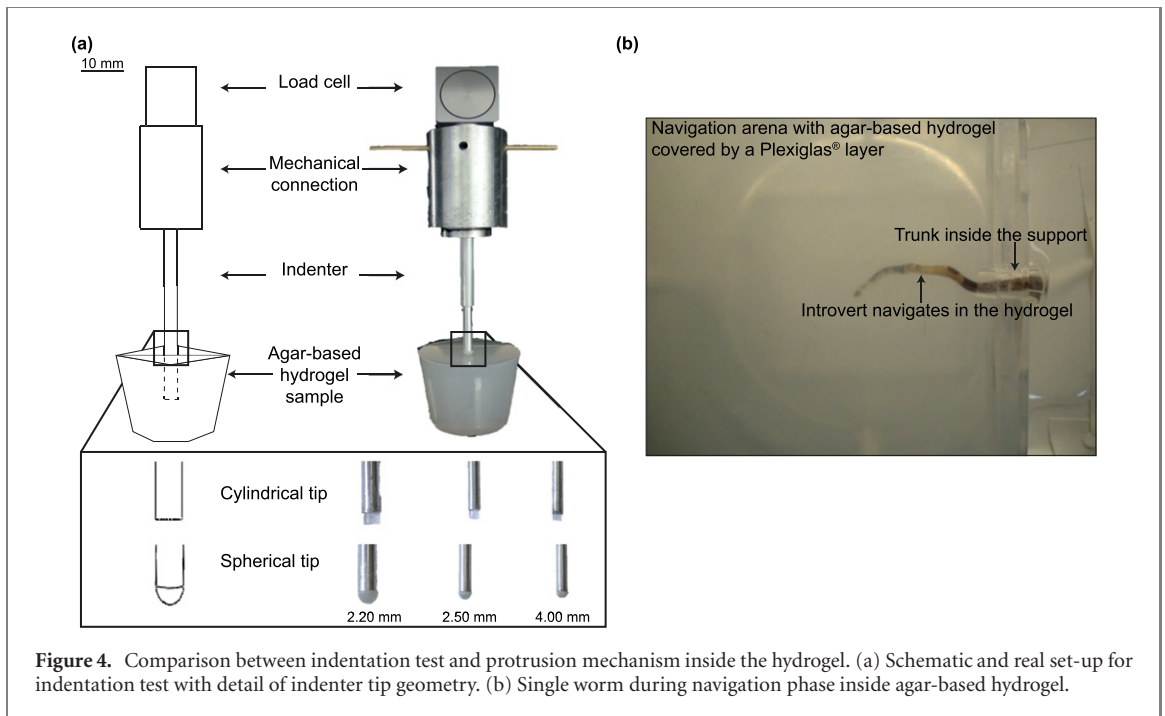


Figure 4. Comparison between indentation test and protrusion mechanism inside the hydrogel. (a) Schematic and real set-up for indentation test with detail of indenter tip geometry. (b) Single worm during navigation phase inside agar-based hydrogel.

assuming as negligible the displacement along the z -axis. Indeed, since the worms were submerged within the navigation medium, the maximum out-of-plane displacement possible equalled the thickness of the navigation arena (i.e. 3 mm), which is significantly lower with respect to the displacement allowed along the x and y directions.

Starting from the x - y coordinates of the virtual markers, the software provided also the x and y velocity components of each marker by using the finite difference algorithm. The data obtained from the tracking software were imported and analysed with MATLAB software (version 9.5, The MathWorks Inc., Natick, MA, USA) and both the kinematic parameters and the exerted forces were evaluated following the lengthening of the introvert. Moreover, by studying the trajectories and the velocity trend of the introvert during the elongation and retraction phases, it was possible to derive the worm elongation percentage (e), defined as:

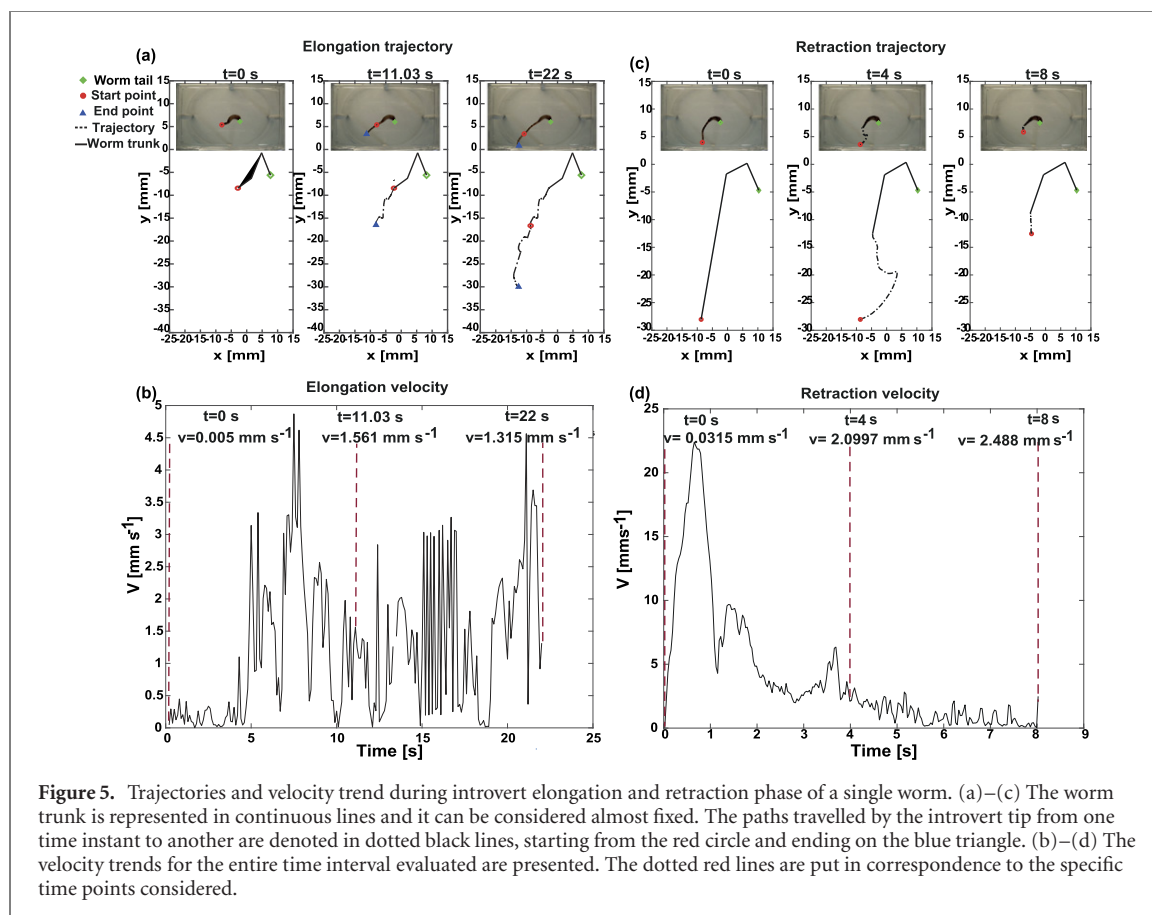
$$e = \frac{L_f - L_0}{L_0} \times 100. \quad (1)$$

where L_f was the maximum worm length and L_0 was the initial one. For each worm, we considered six protrusion events, by analysing the video segments where the worm passed from the defence (i.e. when the introvert is completely folded inside the trunk and its length is L_0) to the protrusion configuration (i.e. when the mouth and the tentacles are exposed and the introvert length is L_f). Mean value and standard deviation of the elongation percentages were calculated per each group.

2.3. Force characterization

Direct and indirect methods can be used for force evaluation. In the first case, dedicated force, pressure or strain sensors are mounted on the navigation arena to detect the forces exerted during locomotion. However, the inclusion of such sensors in confined workspaces is not trivial and the sensors could interfere with the natural behaviour of the organism. In the specific case of sipunculids, the presence of well-developed tactile receptors on the introvert [34] and their non-burrowing behaviour, inhibited the organism from directly pushing against a sensorized wall. For this reason, we decided to opt for indirect force measurements relying on *P. stephensoni* ability to elongate into specific media with known mechanical properties. Agar-based hydrogels were selected to this aim. Hydrogels can be defined as three-dimensional polymeric network structures able to absorb and retain considerable amounts of water [52]. Since the main element is water, these materials present low elastic modulus [53], thus allowing worms to elongate easily inside them.

Indirect force measures were performed by studying the worm elongation capabilities into agar hydrogels featured by different mechanical properties, thus requiring a different force to break the surface and penetrate the medium. In order to tune the gel mechanical properties, different agar (Sigma-Aldrich, St. Louis, MO, USA) concentrations (0.8, 1.0, 1.2, 1.5, 1.7, 2.0% w/v in water) were investigated. Agar hydrogels were prepared in sea water at 90 °C to enable proper powder dissolution also for high concentrations. The solution was poured into cylindrical molds (diameter 37 mm, height 30 mm) and cooled down



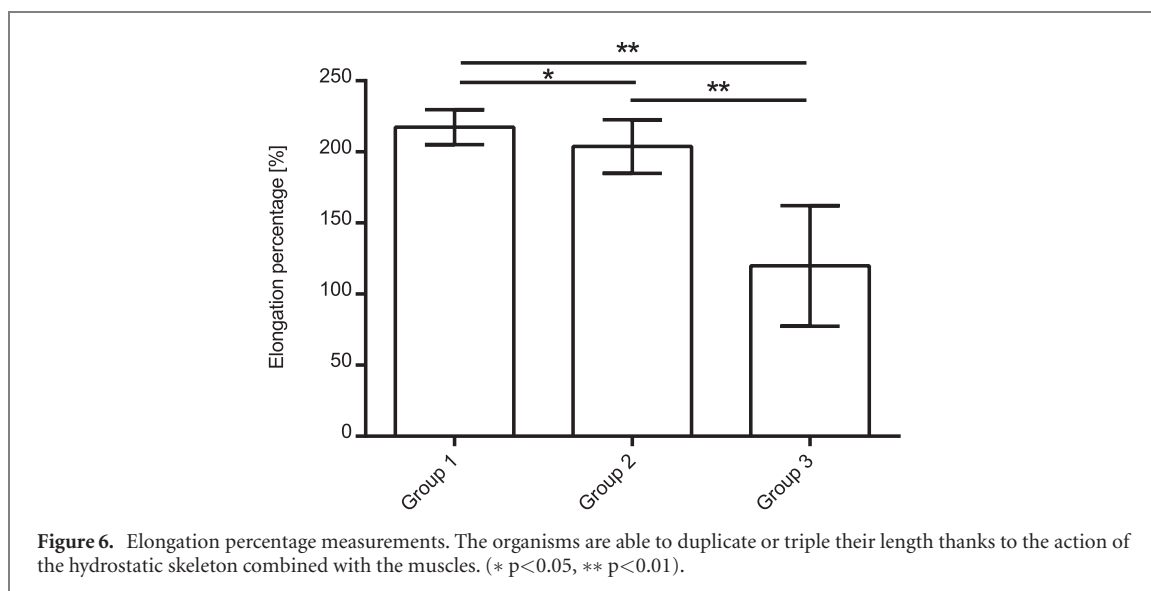
at room temperature for allowing material gelling. In order to study the hydrogel mechanical properties, the samples (five for each indenter diameter) were subjected to indentation test. By definition, the indentation test is a local version of a compression test, where the sample is compressed in a small region instead of across the entire surface [54]. It is a simple and particularly useful technique for mechanically characterizing soft materials, mainly because it does not require sample gripping as in tensile tests [55]. Despite the simplicity of the procedure, it is not straightforward to extract the parameters that describe the soft materials since several factors, such as viscoelasticity and time-dependence, influence their response.

In our case, indentation tests were performed in displacement-control on an Instron[®] Materials Testing Machine (Instron[®], 5900 series, scientific & technical instruments, Canton, Massachusetts, USA) by attaching the indenters to ± 10 N load cell (figure 4(a)). In order to describe the shape variability of the worm tip during the eversion, two different geometries for the indenter were selected (cylindrical and spherical shape). We supposed that the contact edges (and the contact area) between the introvert and the medium vary from the smooth edges of the spherical shape to the sharper and more defined of the cylindrical one [56]. For each geometry three diameters were considered in analogy with the worm groups. The tests were performed at a speed of 1 mm s^{-1} (considered representative for the three

groups) with a stroke of 20 mm inside the gel sample. The values of all the aforementioned parameters were chosen in order to properly replicate the features of the introvert during the elongation.

The obtained data enabled to characterize the gel mechanical properties for different agar compositions. The response curve of the material is a function of the indenter displacement and force. Curve fitting allowed to derive the law correlating displacement and penetration force of the specimen.

Unlike the protrusion characterization, force characterization arena included an additional support to favour protrusion in the frontal direction. By constraining worm trunk, this support could act as a fulcrum to exert greater forces as it happens in the natural environment with the rocks (figure 4(b)). By following the same methodology as in the kinematics characterization, we tracked the coordinates of the specimen tip up to its maximum protrusion. Starting from the measure of the displacement, we could derive the protrusion force based on the constitutive equation obtained from gel indentation tests. In particular, according to the mechanical properties of the material, we evaluated both peak (required to break the medium) and navigation force (required to navigate within the medium). Forces were evaluated for all the nine worms across the six different agar hydrogel concentrations. Each group was let move in all the hydrogels featured by different concentrations: by identifying the stiffer hydrogel where the



worm was able to elongate in, we could derive the maximum protrusion force. Lastly, the force values obtained were used to calculate the stresses required to move inside the material as the ratio of force and cross-sectional area of the worm tip.

3. Results

3.1. Kinematics evaluation

In order to verify the volume invariability, for each organism the volume measurements were carried out before and after the introvert elongation. The assessment through test-tube containing a known volume of water was confirmed by the video analysis which revealed volume mean values of $130.33 \pm 16.82 \text{ mm}^3$ for group 1, $49.43 \pm 6.23 \text{ mm}^3$ and $32.88 \pm 4.81 \text{ mm}^3$ for group 2 and group 3, respectively. The volume difference between defence and protrusion configuration was always below 15%. We believe that these variations could be ascribed to 2D based volume calculations and not linked to real volume fluctuations (table 1).

The characterization results were obtained using the custom experimental set-up (figure 3) and seawater as navigation medium. When the worms were placed inside the custom set-up, their initial posture was of defence, so their body length was minimum and introvert was mostly completely retracted. The worms began to extrude the introvert through a gradual lengthening, in order to explore the surroundings looking for food or shelter and the movement was completely irregular in direction and frequency. The trajectory was mainly marked on the x - y plane by keeping the trunk almost fixed (figure 5(a)) and the protrusion speed varied significantly (figure 5(b)). For the specific specimen reported, representative for all worms, the velocity reached values between 0.5 mm s^{-1} and 5 mm s^{-1} . Conversely, the retraction mechanism was faster than the elongation one. In

particular, initially a high-speed movement occurred with a speed up to 20 mm s^{-1} , followed by a rapid speed fall ending in the complete retraction of the introvert (figure 5(d)).

In this study, we analysed only the maximum worm elongation with respect to the initial configuration. After the calculation of the initial and final body length through the marker's coordinates, we applied (1) to quantify the elongation percentage. Results show that maximum elongation percentage considerably increased with specimen's dimensions. The general overview is that the average elongation percentages spanned from $119 \pm 42\%$ (group 3) to $217 \pm 12\%$ (group 1), passing through $203 \pm 18\%$ for group 2.

A statistical t-test was performed to identify significant differences between the groups to assess whether elongation performances were dependent on the worm body dimension. The differences between groups were statistically significant and suggested that there was a correlation between elongation percentage and organism dimensions ($p = 0.03$ between group 1 and group 2 and $p < 0.001$ both between group 1 and group 3 and between group 2 and group 3) (figure 6).

3.2. Material properties and forces measurements

The mechanical behaviour of the hydrogels was quantified through force–displacement curves. The force–displacement trend can be divided into two regions. The first corresponds to the compression of the material by the indenter until reaching the breaking point, namely the peak force. The second region corresponds to material stress relaxation (namely when the material reaches a lower state of energy and lower forces are needed to move inside) and features a sharp force decrease occurs until reaching a constant value. Curves obtained from cylindrical and spherical indenters were compared (figure 7(a)) revealing that cylindrical indenters reach higher peak forces in

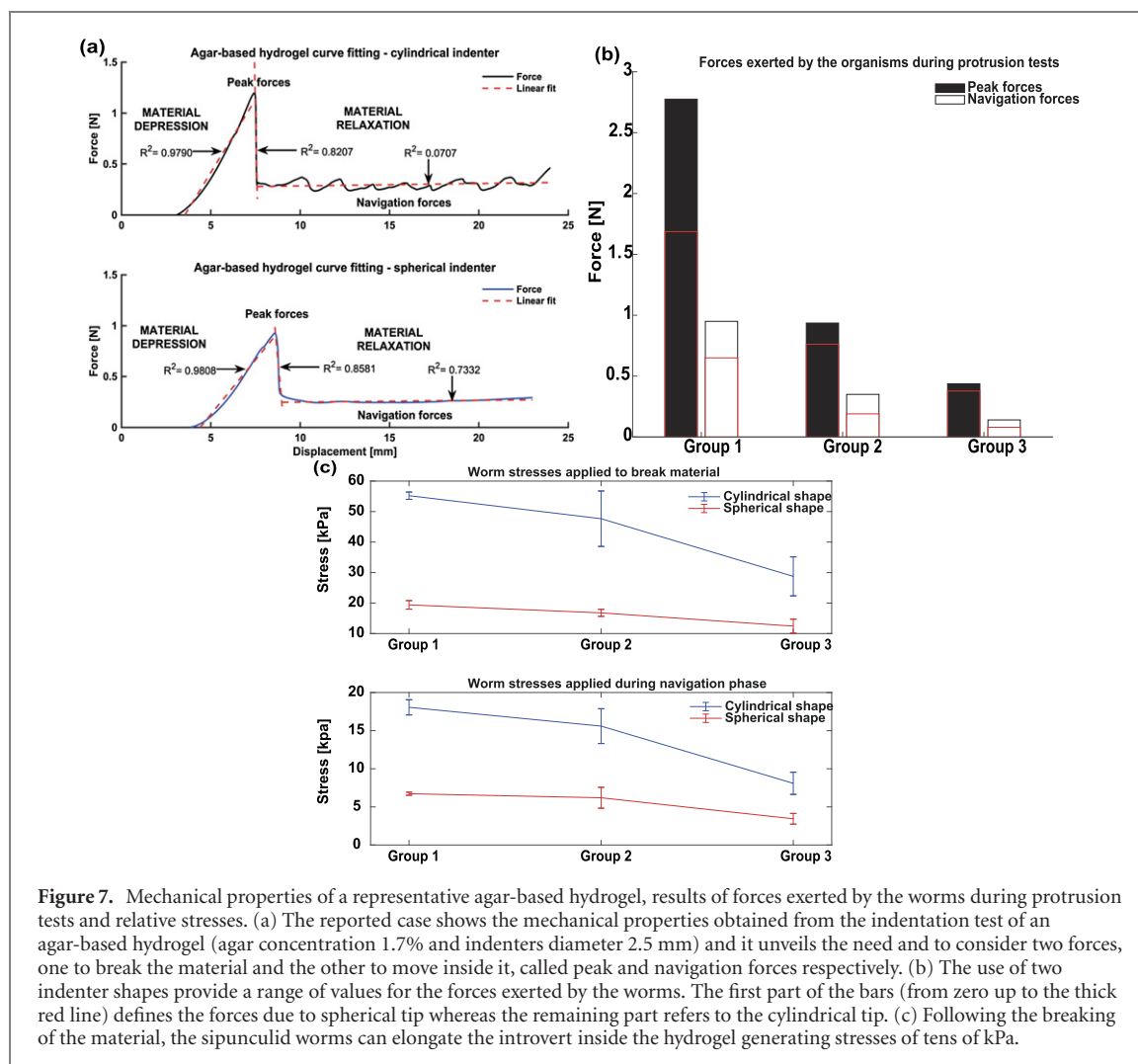


Figure 7. Mechanical properties of a representative agar-based hydrogel, results of forces exerted by the worms during protrusion tests and relative stresses. (a) The reported case shows the mechanical properties obtained from the indentation test of an agar-based hydrogel (agar concentration 1.7% and indenters diameter 2.5 mm) and it unveils the need and to consider two forces, one to break the material and the other to move inside it, called peak and navigation forces respectively. (b) The use of two indenter shapes provide a range of values for the forces exerted by the worms. The first part of the bars (from zero up to the thick red line) defines the forces due to spherical tip whereas the remaining part refers to the cylindrical tip. (c) Following the breaking of the material, the sipunculid worms can elongate the introvert inside the hydrogel generating stresses of tens of kPa.

less time. On the contrary, spherical indenters produced more linear navigation force trends as confirmed by R^2 values closer to one. This trend can be explained with the different relaxation phenomenon for the two tips [55]. Moreover, we reported the forces mean values and their standard deviation resulting from hydrogels characterization with the two types of indenter, at the peak point and during the material relaxation, respectively (table 2).

By testing the capability of the three different sipunculid groups to penetrate into and navigate across media with different mechanical properties, we derived by comparison the peak and navigation force of each group. The data obtained from hydrogels indentation tests showed that the peak forces range between 0.3 N and 2.7 N whereas the navigation forces reach values between 0.08 N and 1.0 N, depending on the agar concentration and on the shape of the indenter.

Protrusion tests within agar media revealed that the worms from all the groups had the ability to navigate across agar gel with concentrations 0.8% and 1.0%.

Samples from group 1 moved smoothly within agar gels with concentrations up to 1.7% (peak force between 1.69 ± 0.14 N and 2.78 ± 0.06 N, navigation force between 0.68 ± 0.03 N and 0.91 ± 0.05 N), whereas they were not able to break the medium in tests with 2% agar. The same applied to group 2 and group 3 which elongated into hydrogels up to 1.5% (peak force between 0.76 ± 0.04 N and 0.94 ± 0.18 N, navigation force 0.24 ± 0.05 N and 0.31 ± 0.04 N) and 1.0% (peak force 0.38 ± 0.07 N and 0.44 ± 0.09 N, navigation force 0.10 ± 0.02 N and 0.12 ± 0.02 N), respectively.

Overall, data analysis reveals that, in order to fracture the material, animals produced average forces between 0.3 N and 2.8 N depending on their dimensions. Average navigation forces were few hundreds of mN (between 0.05 N and 1 N) for all groups, without any significant differences (figure 7(b)).

Assuming the navigation medium as a continuum body and considering the forces depending on the tip area, we calculated the stresses (peak and navigation) value for each group (figure 7(c)) and listed them in table 3.

Table 2. Peak and navigation forces of the agar-based hydrogel obtained from indentation tests. For each diameter (ϕ) of the two indenter shapes (C = cylindrical, S = spherical), five samples were tested and the mean value and standard deviation of the forces were calculated.

Indenter ϕ (mm)	Shape	Agar concentration					
		Peak force (N)	Navigation force (N)	Peak force (N)	Navigation force (N)	Peak force (N)	Navigation force (N)
		0.8%		1.0%		1.2%	
4.00	C	0.693 \pm 0.103	0.253 \pm 0.042	1.173 \pm 0.056	0.352 \pm 0.040	1.475 \pm 0.010	0.533 \pm 0.066
	S	0.450 \pm 0.029	0.149 \pm 0.011	0.860 \pm 0.086	0.268 \pm 0.023	1.248 \pm 0.029	0.389 \pm 0.020
2.50	C	0.384 \pm 0.013	0.127 \pm 0.004	0.645 \pm 0.058	0.177 \pm 0.012	0.754 \pm 0.0075	0.260 \pm 0.023
	S	0.307 \pm 0.088	0.091 \pm 0.009	0.506 \pm 0.054	0.151 \pm 0.006	0.716 \pm 0.045	0.189 \pm 0.030
2.20	C	0.334 \pm 0.016	0.09 \pm 0.004	0.540 \pm 0.042	0.146 \pm 0.009	0.749 \pm 0.009	0.192 \pm 0.016
	S	0.304 \pm 0.004	0.082 \pm 0.003	0.451 \pm 0.011	0.127 \pm 0.010	0.637 \pm 0.085	0.193 \pm 0.009
		1.5%		1.7%		2.0%	
4.00	C	2.410 \pm 0.059	0.793 \pm 0.035	2.775 \pm 0.061	0.908 \pm 0.046	2.635 \pm 0.005	0.943 \pm 0.059
	S	1.688 \pm 0.170	0.581 \pm 0.006	1.687 \pm 0.143	0.676 \pm 0.027	1.706 \pm 0.065	0.833 \pm 0.054
2.50	C	1.118 \pm 0.083	0.352 \pm 0.019	1.224 \pm 0.059	0.457 \pm 0.010	1.409 \pm 0.164	0.459 \pm 0.021
	S	0.808 \pm 0.002	0.298 \pm 0.045	1.054 \pm 0.049	0.386 \pm 0.020	0.923 \pm 0.073	0.408 \pm 0.008
2.20	C	0.849 \pm 0.058	0.274 \pm 0.019	1.107 \pm 0.049	0.345 \pm 0.020	1.130 \pm 0.042	0.370 \pm 0.010
	S	0.800 \pm 0.053	0.253 \pm 0.0052	0.888 \pm 0.035	0.341 \pm 0.008	0.967 \pm 0.076	0.348 \pm 0.020

Table 3. Peak and navigation stress of the organisms obtained from protrusion tests. Based on the forces exerted during the tests, the ratio between forces and cross-sectional area was evaluated for each group of worms.

Group	Maximum agar concentration penetrated (%)	Shape	Peak stress (kPa)	Navigation stress (kPa)
1	1.7	C	55.2 \pm 1.2	18.1 \pm 1.0
		S	19.4 \pm 1.2	6.7 \pm 0.2
2	1.5	C	47.7 \pm 0.9	15.6 \pm 2.3
		S	16.8 \pm 1.4	6.2 \pm 1.4
3	1.0	C	28.8 \pm 6.4	8.1 \pm 1.5
		S	12.4 \pm 2.3	3.4 \pm 0.7

4. Discussions

The main goal of this work was to characterize the protrusion performances (in terms of elongation and forces exerted) of the marine worm *P. stephensoni*, a sipunculid species never characterized to this extent so far. From the literature, it is known that sipunculids have a simplified structure, capable of implementing complex strategies such as performing tasks by lengthening and shape morphing of their body. However, their behaviour and the relation with the worm biomechanics have never been studied before. Synergistic efforts from biologists and engineers are needed to investigate more in detail the behaviour of these organisms in order to derive inspiration and design guidelines for bioinspired robotic artifacts. In general, the values obtained from characterization studies may be a reference to choose the materials to be used or to set the working principles of synthetic machines [57, 58]. Additionally, in our case, unveiling the mechanisms regulating the operation of the hydrostatic skeleton and the introvert protrusion, could be beneficial for developing a novel generation of linear actuators and soft robots able to change their

shapes for navigating the environment [59] and, e.g., for medical applications [60, 61].

A marker-less video tracking system combined with different navigation media enabled for the first time to describe quantitatively both the kinematics of specimens of *P. stephensoni*, when they were completely free to move in seawater without any constraint, and the protrusion force exerted, when navigating across agar-based hydrogels. The uniqueness of sipunculids does not lie in a net movement but in the introvert extrusion, which can be explained by variations in the internal pressure generated by the contraction of circular muscles, own property of the hydrostatic skeleton.

These worms showed an elongation percentage between 100 and 250%, meaning that they can double or almost triple their length based on their dimensions, in accordance with the dependence of biomechanics on size [12]. Indeed, previous studies on the segmented earthworm *Lumbricus terrestris* reported how animal traits and behaviour (i.e. geometry, kinematics, mechanics, burrowing forces) can vary with the scaling of hydrostatic skeleton [41]. From our observations we can deduce that the size affected also the performance of *P. stephensoni*, although its

dimension is smaller than the earthworm and has a continuous and non-segmented body.

Moreover, it is well known that all animals during their movement interact with the environment by exchanging forces; various approaches to quantify them have been suggested. For instance, Quillin has measured the radial and axial forces of *L. terrestris* through a dedicated force-measuring apparatus containing a cylindrical force transducer [62]. On the other hand, Trueman and Foster-Smith were able to measure the internal pressure of *S. nudus* in a direct and invasive way [37]. Although *S. nudus* and *P. stephensoni* belong to the same taxonomic group, the morphology and behaviour of the two species differ significantly due to different ecological requirements thus supporting the importance of the results reported in this paper.

Albeit a direct measurement of force can be more accurate, our characterization study aimed at quantifying forces indirectly. Dorgan and co-workers reported a new method to estimate the forces exerted during digging in artificial sediments by different burrowing annelid species [47–50]. Accordingly, we determined the strength produced by *P. stephensoni* by correlating the desired forces with the mechanical properties of the material. However, our procedure differed from the one proposed by Dorgan and co-workers both for the animal model and for methods (relying on photoelastic stress analysis in the cited work). Despite the proposed methods imply non-natural conditions for the worms, we found out that they were able to easily extrude the introvert even though submerged in a viscous medium. This means that the organisms were able to overcome material's resistance allowing us to shed a light on the forces and stresses these organisms are able to produce when navigating inside the medium.

Starting from hydrogel indentation tests, the use of the two indenter shapes provided us a range of values for the forces exerted by the worms, taking into account the flexibility and the change of the introvert's surface during the protrusion.

For the same reason, starting from peak and navigation forces exerted by the worms, we found a range of values for stresses. It is interesting to note that their average values decrease among groups but no significant differences occur between them. However, it is important to underline that the stress values obtained by indentation tests represent a possible overestimation compared to the stresses generated by living organisms. Indeed, during indentation tests all points of the indenter move inside the medium with constant speed and contact area, whereas this is not the case during introvert eversion, due to the gradual eversion process from the tip.

In conclusion, thanks to the methodologies presented in this work, we were able to reconstruct the trajectory and kinematics of *P. stephensoni* without

the markers' invasiveness. Moreover, we could determine *in vivo* quantitative performance data that cannot be obtained from simple observational methods and we believe that our method could be a good starting point for future biological studies.

Although the knowledge about this sipunculid species is still limited, we are confident that the present findings could have important implications in the robotics field, as initial step towards the development of robotic systems able to replicate the sipunculids' protrusion mechanism and to implement deployment strategies in small-scale devices.

Acknowledgments

This work is part of the PhD thesis of the first author, carried out in collaboration between Scuola Superiore Sant'Anna (Pisa) and Stazione Zoologica Anton Dohrn (Naples). The authors received no external funding. All applicable international, national and/or institutional guidelines for sampling, care and experimental use of organisms for the study have been followed and no particular approvals were necessary.

Conflict of interest

The authors declare no conflict of interest.

ORCID iDs

Silvia Filogna  <https://orcid.org/0000-0001-6358-5649>

Veronica Iacovacci  <https://orcid.org/0000-0002-4052-3581>

Fabrizio Vecchi  <https://orcid.org/0000-0002-8546-0246>

Luigi Musco  <https://orcid.org/0000-0003-4750-4129>

Arianna Mencias  <https://orcid.org/0000-0001-6348-1081>

References

- [1] Yang G-Z *et al* 2018 The grand challenges of science robotics *Sci. Robot.* **3** eaar7650
- [2] Walker I D, Choset H and Chirikjian G S 2016 Snake-like and continuum robots *Springer Handbook of Robotics* (Berlin: Springer) pp 481–98
- [3] Burgner-Kahrs J, Rucker D C and Choset H 2015 Continuum robots for medical applications: a survey *IEEE Trans. Robot.* **31** 1261–80
- [4] Hu X, Chen A, Luo Y, Zhang C and Zhang E 2018 Steerable catheters for minimally invasive surgery: a review and future directions *Comput. Assist. Surg.* **23** 21–41
- [5] Brusca R C and Brusca G J 2003 *Invertebrates* (Basingstoke: Sinauer Press) (no. QL 362. B78 2003) 2 936
- [6] Gray J 1939 Studies in animal locomotion: VIII. The kinetics of locomotion of *Nereis diversicolor* *J. Exp. Biol.* **16** 9–17
- [7] Gray J 1968 *Animal Locomotion* (London: Norton)
- [8] Trueman E R 1975 *Locomotion of Soft-Bodied Animals* (London: Edward Arnold)

- [9] Elder H Y and Trueman E R 1980 *Aspects of Animal Movement (Society for Experimental Biology, Seminar Series vol 5)* (Cambridge: Cambridge University Press)
- [10] Keller J B and Falkovitz M S 1983 Crawling of worms *J. Theor. Biol.* **104** 417–42
- [11] Alexander R McN 1983 *Animal Mechanics* (Oxford: Blackwell) 1985
- [12] Quillin K 1998 Ontogenetic scaling of hydrostatic skeletons: geometric, static stress and dynamic stress scaling of the earthworm *Lumbricus terrestris* *J. Exp. Biol.* **201** 1871–83
- [13] Phee L, Accoto D, Menciassi A, Stefanini C, Carrozza M C and Dario P 2002 Analysis and development of locomotion devices for the gastrointestinal tract *IEEE Trans. Biomed. Eng.* **49** 613–6
- [14] Accoto D, Castrataro P and Dario P 2004 Biomechanical analysis of Oligochaeta crawling *J. Theor. Biol.* **230** 49–55
- [15] Wang K D and Yan G Z 2006 An earthworm-like microrobot for colonoscopy *Biomed. Instrum. Technol.* **40** 471–8
- [16] Spina G L, Sfakiotakis M, Tsakiris D P, Menciassi A and Dario P 2007 Polychaete-like undulatory robotic locomotion in unstructured substrates *IEEE Trans. Robot.* **23** 1200–12
- [17] Shin B H, Choi S-W, Bang Y-B and Lee S-Y 2011 An earthworm-like actuator using segmented solenoids *Smart Mater. Struct.* **20** 105020
- [18] Song C-W, Lee D-J and Lee S-Y 2016 Bioinspired segment robot with earthworm-like plane locomotion *J. Bionic Eng.* **13** 292–302
- [19] Wang K, Yan G, Ma G and Ye D 2009 An earthworm-like robotic endoscope system for human intestine: design, analysis, and experiment *Ann. Biomed. Eng.* **37** 210–21
- [20] Chowdhury A, Ansari S and Bhaumik S 2017 Earthworm like modular robot using active surface gripping mechanism for peristaltic locomotion *Proc. of the Advances in Robotics* pp 1–6
- [21] Choi H et al 2002 Microrobot actuated by soft actuators based on dielectric elastomer *IEEE/RSJ Int. Conf. on Intelligent Robots and Systems* vol 2 (IEEE) pp 1730–5
- [22] Menciassi A, Gorini S, Pernorio G and Dario P 2004 A SMA actuated artificial earthworm *Proc. of the IEEE Int. Conf. on Robotics and Automation (ICRA'04)* vol 4 (IEEE) pp 3282–7
- [23] Menciassi A, Accoto D, Gorini S and Dario P 2006 Development of a biomimetic miniature robotic crawler *Auton. Robot.* **21** 155–63
- [24] Jung K, Koo J C, Nam J-d., Lee Y K and Choi H R 2007 Artificial annelid robot driven by soft actuators *Bioinspir. Biomim.* **2** S42
- [25] Seok S, Onal C D, Cho K-J, Wood R J, Rus D and Kim S 2012 Meshworm: a peristaltic soft robot with antagonistic nickel titanium coil actuators *IEEE/ASME Trans. Mechatronics* **18** 1485–97
- [26] Phee L, Menciassi A, Accoto D, Stefanini C and Dario P 2003 Analysis of robotic locomotion devices for the gastrointestinal tract *Robotics Research* (Berlin: Springer) pp 467–83
- [27] Zuo J, Yan G and Gao Z 2005 A micro creeping robot for colonoscopy based on the earthworm *J. Med. Eng. Technol.* **29** 1–7
- [28] Mangan E V, Kingsley D A, Quinn R D and Chiel H J 2002 Development of a peristaltic endoscope *Proc. 2002 IEEE Int. Conf. on Robotics and Automation (Cat. No. 02CH37292)* vol 1 (IEEE) pp 347–52
- [29] Zarrouk D and Shoham M 2012 Analysis and design of one degree of freedom worm robots for locomotion on rigid and compliant terrain *J. Mech. Des.* **134** 021010
- [30] Calderón A A, Ugalde J C, Chang L, Zagal J C and Pérez-Arancibia N O 2019 An earthworm-inspired soft robot with perceptive artificial skin *Bioinspir. Biomim.* **14** 056012
- [31] Joey Z G, Calderón A A, Chang L and Pérez-Arancibia N O 2019 An earthworm-inspired friction-controlled soft robot capable of bidirectional locomotion *Bioinspir. Biomim.* **14** 036004
- [32] Tang Z, Lu J, Wang Z, Chen W and Feng H 2019 Design of a new air pressure perception multi-cavity pneumatic-driven earthworm-like soft robot *Auton. Robot.* **44** 1–13
- [33] Zhao Y, Shan Y, Zhang J, Guo K, Qi L, Han L and Yu H 2019 A soft continuum robot, with a large variable-stiffness range, based on jamming *Bioinspir. Biomim.* **14** 066007
- [34] Cutler E B 2018 *The Sipuncula (Their Systematics, Biology, and Evolution)* (Ithaca, NY: Cornell University Press)
- [35] Zuckerkandl E 1950 Coelomic pressures in *Sipunculus nudus* *Biol. Bull.* **98** 161–73
- [36] Murina G-V 1984 Ecology of *Sipuncula* *Mar. Ecol. Prog. Ser.* **17** 1–7
- [37] Trueman E and Foster-Smith R 1976 The mechanism of burrowing of *Sipunculus nudus* *J. Zool.* **179** 373–86
- [38] Li J, Zhu C, Guo Y, Xie X, Huang G and Chen S 2015 Experimental study of bioturbation by *Sipunculus nudus* in a polyculture system *Aquaculture* **437** 175–81
- [39] Chapman G 1958 The hydrostatic skeleton in the invertebrates *Biol. Rev.* **33** 338–71
- [40] Yekutieli Y, Mitelman R, Hochner B and Flash T 2007 Analyzing octopus movements using three-dimensional reconstruction *J. Neurophysiol.* **98** 1775–90
- [41] Kurth J A and Kier W M 2014 Scaling of the hydrostatic skeleton in the earthworm *Lumbricus terrestris* *J. Exp. Biol.* **217** 1860–7
- [42] Hedrick T L 2008 Software techniques for two- and three-dimensional kinematic measurements of biological and biomimetic systems *Bioinspir. Biomim.* **3** 034001
- [43] Quillin K J 1999 Kinematic scaling of locomotion by hydrostatic animals: ontogeny of peristaltic crawling by the earthworm *Lumbricus terrestris* *J. Exp. Biol.* **202** 661–74
- [44] Saga N and Nakamura T 2004 Development of a peristaltic crawling robot using magnetic fluid on the basis of the locomotion mechanism of the earthworm *Smart Mater. Struct.* **13** 566
- [45] Waldron K J, Omori H, Nakamura T and Yada T 2009 An underground explorer robot based on peristaltic crawling of earthworms *Industrial Robot: An International Journal* **36** 358–64
- [46] Kwon N, Pyo J, Lee S-J and Je J H 2013 3D worm tracker for freely moving *C. elegans* *PLoS One* **8** e57484
- [47] Dorgan K M, Jumars P A, Johnson B, Boudreau B P and Landis E 2005 Burrow extension by crack propagation *Nature* **433** 475
- [48] Dorgan K M, Arwade S R and Jumars P A 2007 Burrowing in marine muds by crack propagation: kinematics and forces *J. Exp. Biol.* **210** 4198–212
- [49] Murphy E A K and Dorgan K M 2011 Burrow extension with a proboscis: mechanics of burrowing by the glycerid *Hemipodus simplex* *J. Exp. Biol.* **214** 1017–27
- [50] Grill S and Dorgan K M 2015 Burrowing by small polychaetes-mechanics, behavior and muscle structure of *Capitella* sp *J. Exp. Biol.* **218** 1527–37
- [51] Ferrero-Vicente L, Rubio-Portillo E and Ramos-Esplá A 2016 *Sipuncula* inhabiting the coral *Oculina patagonica* in the western Mediterranean Sea *Marine Biodiversity Records* **9** 2
- [52] Rosiak J M and Yoshii F 1999 Hydrogels and their medical applications *Nucl. Instrum. Meth. B* **151** 56–64
- [53] Rattan S, Li L, Lau H K, Crosby A J and Kiick K L 2018 Micromechanical characterization of soft, biopolymeric hydrogels: stiffness, resilience, and failure *Soft matter* **14** 3478–89
- [54] Oyen M L 2014 Mechanical characterisation of hydrogel materials *Int. Mater. Rev.* **59** 44–59
- [55] Galli M, Comley K S C, Shean T A V and Oyen M L 2009 Viscoelastic and poroelastic mechanical characterization of hydrated gels *J. Mater. Res.* **24** 973–9
- [56] Oyen M L 2013 Nanoindentation of biological and biomimetic materials *Exp. Tech.* **37** 73–87

- [57] Margheri L, Laschi C and Mazzolai B 2012 Soft robotic arm inspired by the octopus: I. From biological functions to artificial requirements *Bioinspir. Biomim.* **7** [025004](#)
- [58] Luo Y, Zhao N, Wang H, Kim K J and Shen Y 2017 Design, modeling and experimental validation of a scissor mechanisms enabled compliant modular earthworm-like robot *IEEE/RSJ Int. Conf. on Intelligent Robots and Systems (IROS 2017)* (IEEE) pp 2421–6
- [59] Hawkes E W, Blumenschein L H, Greer J D and Okamura A M 2017 A soft robot that navigates its environment through growth *Sci. Robot.* **2** [eaaan3028](#)
- [60] Cianchetti M, Ranzani T, Gerboni G, Nanayakkara T, Althoefer K, Dasgupta P and Menciassi A 2014 Soft robotics technologies to address shortcomings in today's minimally invasive surgery: the STIFF-FLOP approach *Soft Robot.* **1** [122–31](#)
- [61] Slade P, Gruebele A, Hammond Z, Raitor M, Okamura A M and Hawkes E W 2017 Design of a soft catheter for low-force and constrained surgery *IEEE/RSJ Int. Conf. on Intelligent Robots and Systems (IROS 2017)* (IEEE) pp 174–80
- [62] Quillin K 2000 Ontogenetic scaling of burrowing forces in the earthworm *Lumbricus terrestris* *J. Exp. Biol.* **203** 2757–70